

Modeling and Control Design for a Bidirectional DC-DC Converter System for Cyclic Operation of a Reversible Solid Oxide Electrolysis Cell Stack

Jessen, Kasper; N. Soltani, Mohsen; Hajizadeh, Amin; Jensen, Søren Højgaard; Schaltz, Erik

Published in:

IECON 2023 - 49th Annual Conference of the IEEE Industrial Electronics Society

DOI (link to publication from Publisher):

[10.1109/IECON51785.2023.10311857](https://doi.org/10.1109/IECON51785.2023.10311857)

Creative Commons License

CC BY 4.0

Publication date:

2023

Document Version

Accepted author manuscript, peer reviewed version

[Link to publication from Aalborg University](#)

Citation for published version (APA):

Jessen, K., N. Soltani, M., Hajizadeh, A., Jensen, S. H., & Schaltz, E. (2023). Modeling and Control Design for a Bidirectional DC-DC Converter System for Cyclic Operation of a Reversible Solid Oxide Electrolysis Cell Stack. In *IECON 2023 - 49th Annual Conference of the IEEE Industrial Electronics Society* Article 10311857 IEEE (Institute of Electrical and Electronics Engineers). <https://doi.org/10.1109/IECON51785.2023.10311857>

General rights

Copyright and moral rights for the publications made accessible in the public portal are retained by the authors and/or other copyright owners and it is a condition of accessing publications that users recognise and abide by the legal requirements associated with these rights.

- Users may download and print one copy of any publication from the public portal for the purpose of private study or research.
- You may not further distribute the material or use it for any profit-making activity or commercial gain
- You may freely distribute the URL identifying the publication in the public portal -

Take down policy

If you believe that this document breaches copyright please contact us at vbn@aub.aau.dk providing details, and we will remove access to the work immediately and investigate your claim.

Modeling and Control Design for a Bidirectional DC-DC Converter System for Cyclic Operation of a Reversible Solid Oxide Electrolysis Cell Stack

Kasper Jessen¹, Mohsen Soltani¹, Amin Hajizadeh¹, Søren H. Jensen^{2,3}, Erik Scholtz³

Abstract—This paper presents a design of a bidirectional DC-DC power electronic converter system enabling cyclic operation for a Reversible Solid Oxide Electrolysis Cell (RSOEC) stack for steam electrolysis. The cyclic operation of the RSOEC stack is investigated, and two different equivalent circuit models are presented for the mathematical representation of the stack's electrical dynamics: The well-established steady-state Resistive model and a novel Voigt model. From these, two combined mathematical models of the bidirectional Buck-Boost converter supplying the RSOEC stack are derived using the small-signal averaging technique. For tracking the cyclic output current reference to an RSOEC stack, two Proportional Integral Derivative with derivative Filter (PIDF) controllers are designed using the two combined mathematical models derived. Finally, the performances of the two PIDF controllers for the bidirectional DC-DC converter systems are compared and validated through simulations. The simulation results confirm the bidirectional Buck-Boost converter's ability to deliver cyclic bidirectional output current and demonstrate that the control tuned based on the Voigt mathematical representation of the RSOEC stack yields superior closed-loop performance in accordance with the control design requirements.

Index Terms—Reversible solid oxide electrolyzer cell, Bidirectional DC-DC converter, Control design, Cyclic operation (AC:DC) method

I. INTRODUCTION

The Solid Oxide Cell (SOC) technology has the highest energy efficiency potential for hydrogen production as an electrolyzer and electricity generation as a fuel cell. Furthermore, the same SOC can often be used for both operation modes, denoted as a Reversible Solid Oxide Cell (RSOC). But, the SOC technology suffers high cost and insufficient long-term durability, particularly at high

current densities, which hinders this technology scaling possibility [1], [2]. A novel reversible cyclic operation mode approach has been proposed for Reversible Solid Oxide Electrolyzer Cell (RSOEC) stacks in [3], [4]. The cyclic operation between electrolysis and fuel cell modes on an RSOEC stack was experimentally verified to minimize the degradation of the cells. This could result in a simple way to increase the RSOEC stack size and lifetime.

However, a bidirectional power electronic converter is required to perform the cyclic operation method of the RSOEC. The bidirectional power electronic converters are an enabling technology, as it facilitates the interface between energy storage technologies. Therefore, bidirectional power electronic converters and their control have been a widely researched topic. In [5], an overview of the topologies and the control schemes for bidirectional DC-DC power converters is presented. Electrochemical energy storage technology is widely used, which covers common technologies such as batteries and supercapacitors. However, the advancements for the RSOC have become a viable option for electrochemical energy storage [2]. In [6], a comprehensive review of the different power converter interfaces for electrochemical energy storage systems is presented. It is important for the operation cost that the efficiency of a bidirectional power converter for the RSOEC stack is kept high. However, this task is challenging due to the RSOEC stack voltage having a wide operating range and inhibiting a non-linear current dependency.

Different bidirectional power converter topologies for interfacing with an RSOC stack have been investigated. These include the non-isolated bidirectional DC-DC converter topologies: Buck-Boost Converter (BBC) [7] and interleaved buck-boost converter [8] and the isolated bidirectional DC-DC converter topologies: Isolated full bridge boost converter [9]–[11], dual-active bridge [11]–[13], and cascaded converter structures

*This work is a part of the DynAmmonia and DynEfuel projects both supported by EUDP with grant numbers 64021-3104 and 640222-496142, respectively.

¹ with the dept. AAU Energy, Aalborg University, 6700 Esbjerg, Denmark kje@et.aau.dk

² with the company Dynelectro ApS, 4130 Viby Sjælland, Denmark

³ with the dept. AAU Energy, Aalborg University, 9220 Aalborg, Denmark

[13]–[15]. The cyclic operation of a RSOEC stack imposes additional challenging requirements for the bidirectional DC-DC converter system, such as fast tracking performance during reversible operation mode and properly damped oscillations.

The contributions of this paper are as follows:

- The requirements for efficient operation of the bidirectional DC-DC converter and its control system for the cyclic operation of an RSOEC stack were analyzed.
- The control system to ensure fulfillment of the specified closed-loop dynamic performance requirements for the cyclic operation of an RSOEC stack was designed, using both a resistive ECM and a novel Voigt ECM for the electrical behavior of an RSOEC stack in the design process.
- The dynamic performance of the bidirectional BBC with the two different control in cyclic operation was compared and validated through simulations.

Furthermore, this paper aims to highlight the design challenges for bidirectional power electronic converters for a cyclic-operated RSOEC stacks to promote further research in this area.

This paper is organized as follows. Section II briefly overviews the RSOEC stack and cyclic operation mode. Section III formulates the mathematical model for the BBC converter supplying the Voigt ECM of the RSOEC. Section IV describes the design process for the PIDF controllers for the bidirectional BBC enabling cyclic operation of the RSOEC stack. Section V contains a validation and comparison of the designed PIDF controllers for the bidirectional BBC in cyclic operation through simulations. The last section VI, is the conclusion of the paper.

II. REVERSIBLE SOLID OXIDE CELL

The RSOC consists of three main components: a dense ceramic electrolyte and two porous electrodes. The RSOC operates at a high temperature, around 600–900°C, which results in very high conversion efficiencies due to the theoretical thermodynamic efficiency increases with increasing temperature [2].

A single RSOC is only a few millimeters thick and provides a low cell voltage. Therefore, multiple RSOC are connected in series to provide a higher voltage. The series connection of multiple RSOCs is often referred to as a stack. By increasing the stack size, the voltage and power of the RSOC stack will also increase. This is an advantage as it will decrease the cost per unit output of the stack and will ease the requirement of the conversion ratio for the DC-DC power electronic converter. The disadvantage of increasing the stack size is that temperature variation in the RSOC stack will increase, causing thermomechanical stresses in the stack, which increase

variation in current density, the degradation rate, leak probability, and possibly device failure [16], [17].

Recently, a new operation mode (AC:DC) for Reversible Solid Oxide Electrolyzer Cell (RSOEC) was proposed in [4], which works by rapidly cycling between fuel cell and electrolysis mode, with a cycling time in the order of milliseconds. The cyclic operation was conducted by cycling asymmetrically around the Open-Circuit Voltage (OCV) of the RSOEC stack. The operation method has been experimentally validated and was shown to alleviate temperature variations and minimize degradation caused by impurities and nickel migration.

In this paper, the cyclic operation for an RSOEC stack is considered to occur at a maximum cyclic frequency, f_{cyclic} , of 50 Hz and with a maximum percentage of electrolysis to fuel cell operating time of 90%. The nominal operation is conducted at an output current reference amplitude at 55A in electrolysis mode and 45A in fuel cell mode.

III. MATHEMATICAL MODELLING

To design the control system and analyze the stability of the closed loop system, an adequate mathematical model of the electrical dynamics of both the bidirectional BBC and RSOEC stack is necessary.

The circuit diagram of the bidirectional BBC supplying an RSOEC from a DC-bus can be seen in Fig. 1.

However, there exist different approaches for the RSOEC stack modeling. In previous work conducted in the field of bidirectional DC-DC converter design for an RSOC stack, a unidirectional approach has been applied in [8], [10], [13], [14]. The unidirectional approach applies a voltage source to model the fuel-cell mode and a resistive load in the electrolysis mode. However, a more accurate bidirectional representation is the use of a simple resistive ECM consisting of a voltage source and a resistor, which is dimensioned to model the linearised steady-state characteristics, often visualized in an I-V curve, of the RSOC [9], [11], [12], [15], [18]. The resistive ECM is suitable for capturing the steady-state behavior of the model and is therefore useful for e.g. Steady-state conversion efficiency calculations for PEC. However, due to the cyclic operation method considered

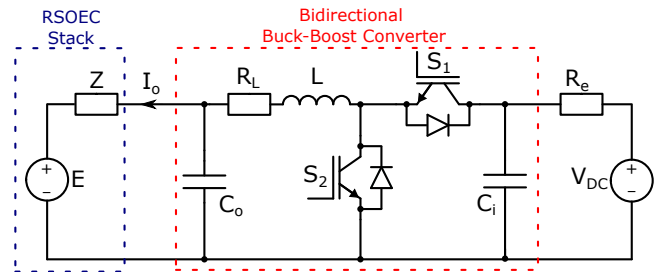


Fig. 1. The circuit diagram for a bidirectional Buck-Boost converter connected to an RSOEC stack.

in this paper, the RSOEC is going to be periodically excited and operate a substantial amount of the time in a transient state. Therefore, a more detailed model is necessary to provide a better representation of the transient electrical dynamics in the mathematical model of the RSOEC.

In a previous paper [19], the author conducted a novel study to model the electrical dynamics for an commercial scale RSOEC stack using an ideal lumped ECM, which was parametrized using a Grey-box modeling approach. The model developed is denoted as the Voigt ECM representation. The parametrization of the Voigt ECM was conducted in the frequency domain, and was based on experimental data collected using electrochemical impedance spectroscopy under different operating conditions at different aging stages. A time domain comparison of the electrical dynamics in cyclic operation mode between the nominal parametrized Voigt ECM in a simulation environment and the commercial RSOEC stack in an experimental environment was conducted at different aging stages. The nominal parametrized Voigt ECM, showed a good agreement in the transient electrical dynamics, however a low steady-state error was observed at early aging states due to the lower ohmic resistances. The nominal parameters for the Voigt ECM derived can be seen in Table I. The Voigt and Resistive ECM representation can be seen in Fig. 2. It should be noted that the Voigt ECM used in this paper has included a small parasitic inductance, mainly due to the wires from PEC to the RSOEC stack, but also includes inductance from the current collectors of the RSOEC. This paper shows only the mathematical model for the plant consisting of the bidirectional BBC in continuous conduction mode supplying an RSOEC stack represented by the Voigt ECM stack. The parameters for the bidirectional BBC and the two ECM for the RSOEC stack can be seen in Table I. The dynamics of the plant can be described by the averaged large-signal differential equations in 1

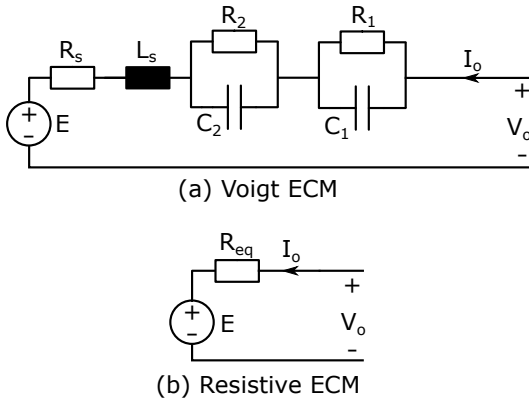


Fig. 2. The two ECM representations for the description of the electrical behavior for an RSOEC stack.

TABLE I
PARAMETERS OF THE BUCK-BOOST CONVERTER IN FIG. 1 AND
RSOEC MODELS IN FIG. 2

Description	Symbol	Value
<u>Converter</u>		
Switching frequency	f_{sw}	100 kHz
Sampling frequency	f_s	50 kHz
Input voltage	v_{DC}	150 V
Input capacitor	C_i	25 μ F
Output capacitor	C_o	50 μ F
Inductor	L	75 μ H
ESR Inductor	R_L	10 m Ω
DC-bus wire resistance	R_e	1 m Ω
<u>ECM</u>		
Voigt ECM capacitor	C_1	0.61 F
Voigt ECM capacitor	C_2	0.47 mF
Voigt ECM resistor	R_1	0.21 Ω
Voigt ECM resistor	R_2	0.15 Ω
Voigt ECM resistor	R_s	0.20 Ω
OCV RSOEC stack	E	61 V
Parasitic stack inductance	L_s	30 nH
Resistive ECM resistor	R_{eq}	0.56 Ω

$$\begin{aligned}
C_1 \frac{dv_{c1}(t)}{dt} &= I_o(t) - \frac{v_{c1}(t)}{R_1} \\
C_2 \frac{dv_{c2}(t)}{dt} &= I_o(t) - \frac{v_{c2}(t)}{R_2} \\
C_i \frac{dv_i(t)}{dt} &= \frac{v_{DC} - v_i(t)}{R_e} - I_L(t)D(t) \\
C_o \frac{dv_o(t)}{dt} &= I_L(t) - I_o(t) \\
L \frac{dI_L(t)}{dt} &= v_i(t)D(t) - v_o(t) - R_L I_L(t) \\
L_s \frac{dI_o(t)}{dt} &= v_o(t) - v_1(t) - v_2(t) - R_s I_o(t) - E(t)
\end{aligned} \tag{1}$$

where v_{c1} and v_{c2} are the voltage across the C_1 and C_2 capacitors, and I_o is the current through the parasitic stack inductance L_s in the Voigt ECM. v_i and v_o are the voltage across the input and output capacitors of the Buck-Boost converter. I_L are the current through the converters inductor L . D is the duty-cycle, which is the ratio of on-time for switch 1 (S_1) to switch 2 (S_2) within one switching cycle.

To utilize the derived plant model for control design, a small signal analysis is needed [20], [21]. The small signal averaged model of the plant is represented in state-space form in 2

$$\begin{aligned}
\mathbf{A} &= \begin{bmatrix} \frac{-1}{C_1 R_1} & 0 & 0 & 0 & 0 & \frac{1}{C_1} \\ 0 & \frac{-1}{C_2 R_2} & 0 & 0 & 0 & \frac{1}{C_2} \\ 0 & 0 & \frac{-1}{C_i R_e} & 0 & \frac{-\bar{D}}{C_i} & 0 \\ 0 & 0 & 0 & 0 & \frac{1}{C_o} & \frac{-1}{C_o} \\ 0 & 0 & \frac{\bar{D}}{L} & \frac{-1}{L} & \frac{-R_L}{L} & 0 \\ \frac{-1}{L_s} & \frac{-1}{L_s} & 0 & \frac{1}{L_s} & 0 & \frac{-R_s}{L_s} \end{bmatrix} \\
\mathbf{B} &= \begin{bmatrix} 0 & 0 & \frac{1}{C_i R_e} & 0 & 0 & 0 \\ 0 & 0 & 0 & 0 & 0 & \frac{1}{L_s} \\ 0 & 0 & \frac{\bar{I}_L}{C_i} & 0 & 0 & \frac{\bar{V}_i}{L} \end{bmatrix}^\top \\
\mathbf{C} &= \begin{bmatrix} 0 & 0 & 0 & 0 & 0 & 1 \end{bmatrix} \\
\mathbf{D} &= \mathbf{0}_{3 \times 3} \\
\mathbf{x}(t) &= \begin{bmatrix} \tilde{v}_{c1}(t) & \tilde{v}_{c2}(t) & \tilde{v}_i(t) & \tilde{v}_o(t) & \tilde{i}_L(t) & \tilde{i}_o(t) \end{bmatrix}^\top \\
\mathbf{u}(t) &= \begin{bmatrix} \tilde{v}_{dc}(t) & \tilde{E}(t) & \tilde{d}(t) \end{bmatrix}^\top \\
y(t) &= \tilde{i}_o(t)
\end{aligned} \tag{2}$$

where the tilde notation in the states indicates small-signal quantities near the linearization point. The linearization point is indicated by the average values of the duty-cycle, input capacitor voltage, and inductor current denoted \bar{D} , \bar{V}_i and \bar{I}_L , respectively.

The small-signal averaged model is suitable for control design, but its accuracy at high frequencies is limited due to the ignorance of high-frequency dynamics. Therefore, a general rule is that the small-signal averaged model should not be applied beyond one-tenth or one-sixth of the switching frequency [22].

The frequency response from the small-signal model of the bidirectional buck-boost converter supplying the two different ECM representing the RSOEC stack at the nominal operating point can be seen in Fig. 3 at the linearization point $\bar{D}=0.79$, $\bar{V}_i=150$ V, and $\bar{I}_L=45$ A.

IV. CONTROL

The proposed control system is designed to fulfil certain control system design requirements given by the control system design engineer. In this paper, these control system design requirements are:

- An underdamped system, with a minimum of oscillations.
- A cut off frequency f_{co} of the system placed in the range of $10 f_{cyclic} < f_{co} < f_s/10$
- A settling time within 20% of the minimum fuel-cell mode operating time.
- A low overshoot of a maximum of 10%.
- A steady-state error within 1%.

To achieve these requirements a PIDF control algorithm is utilized. The PIDF control is one the most common

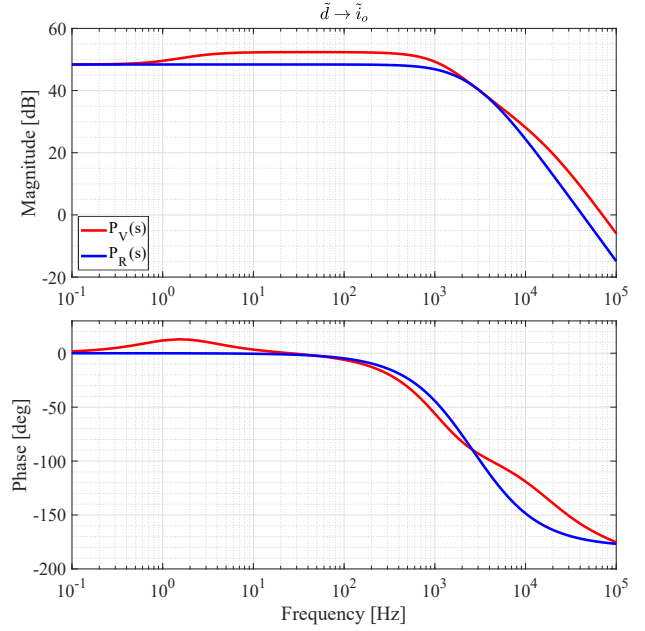


Fig. 3. The bode plots of the two continuous open-loop plants. P_V and P_R are the plants using the Voigt and Resistive ECM, respectively.

control algorithms used in industry and has been universally accepted in various industrial control. The general parallel transfer function of the discrete PIDF controller using the forward Euler method can be seen in 3

$$K(z) = k_p + \frac{k_i T_s}{z-1} + \frac{k_d}{\tau_F + \frac{T_s}{z-1}} \tag{3}$$

where $K(z)$ is the discrete transfer function of the PIDF control algorithm. k_p , k_i , and k_d is the proportional, integral, and derivative term, respectively. τ_F is the time constant for the low-pass filter on the derivative term. The PIDF control algorithm ensures there will be no steady-state error, due to the integral term. However, to fulfil the remaining control design requirements, a control tuning procedure for the PIDF controller was undertaken. A digital control design approach was employed as it is intended to implement the designed control algorithm using software on a microprocessor in future works. For the digital control a discretization of the continuous open-loop plant models was necessary, for this the Zero-Order-Hold (ZOH) method was utilized. The two discrete plant models for the perturbation in duty-cycle to output current can be described by the discrete transfer functions in 4

$$\begin{aligned}
P_V(z) &= \frac{22.8z^5 - 28.5z^4 - 2.9z^3 + 8.6z^2 + 4.1e-4z - 4.7e-22}{z^6 - 2.8z^5 + 2.8z^4 - z^3 + 0.1z^2 - 8.0e-19z - 6.7e-36} \\
P_R(z) &= \frac{12.0z^2 + 9.5z + 5.1e-12}{z^3 - 1.4z^2 + 0.5z}
\end{aligned} \tag{4}$$

TABLE II
PARAMETERS OF THE DISCRETE PIDF CONTROLLERS TUNED
USING THE VOIGT ECM (K_V) AND RESISTIVE ECM (K_R)

	k_p	k_i	k_d	τ_F
$K_V(z)$	6.64×10^{-3}	33.1	4.48×10^{-8}	6.99×10^{-5}
$K_R(z)$	6.36×10^{-3}	46.7	7.54×10^{-8}	5.31×10^{-5}

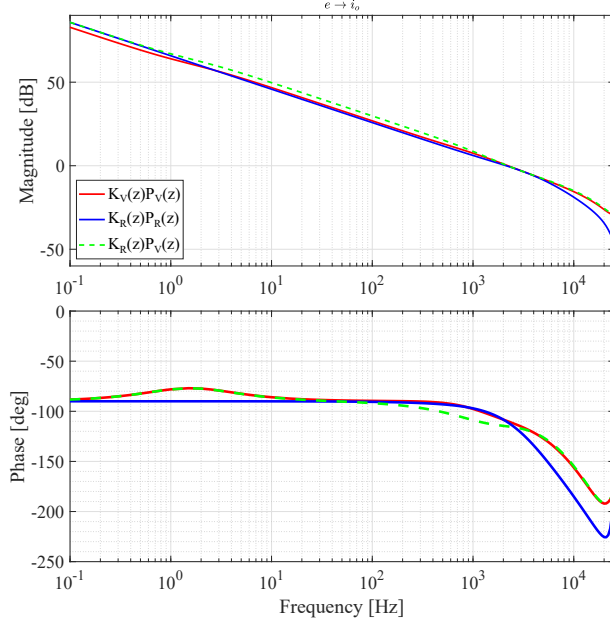


Fig. 4. A bode plots where the solid lines vizulize the discrete open-loop systems with their respective designed discrete controller. The dashed line visualize the Voigt BBC plant with the controller designed for the Resistive ECM.

where $P_V(z)$ and $P_R(z)$ are the discrete plant transfer function of the bidirectional BBC with the Voigt ECM and Resistive ECM, respectively. The tuning of the PIDF controller for the two discrete plant models was conducted via the frequency response utilizing the Bode plot of the open-loop system. The two PIDF controllers was tuned with their individual discrete plant model to achieve a bandwidth of 2 kHz, and a phase margin of 60 degrees. The PIDF control parameters for the two controllers can be seen in Table II.

The open-loop systems with their respective designed controllers can be seen in Fig. 4. The impact of using a simplified Resistive ECM for the RSOEC stack in the control design is visualized, and it can be seen that the phase margin is considerably lowered and the gain is increased at lower frequencies than the cut-off frequency.

V. VALIDATION

To validate and compare the time domain dynamic performance of the bidirectional BBC with two the control systems, a set of simulations is conducted using MATLAB Simulink and the Simscape Electrical library.

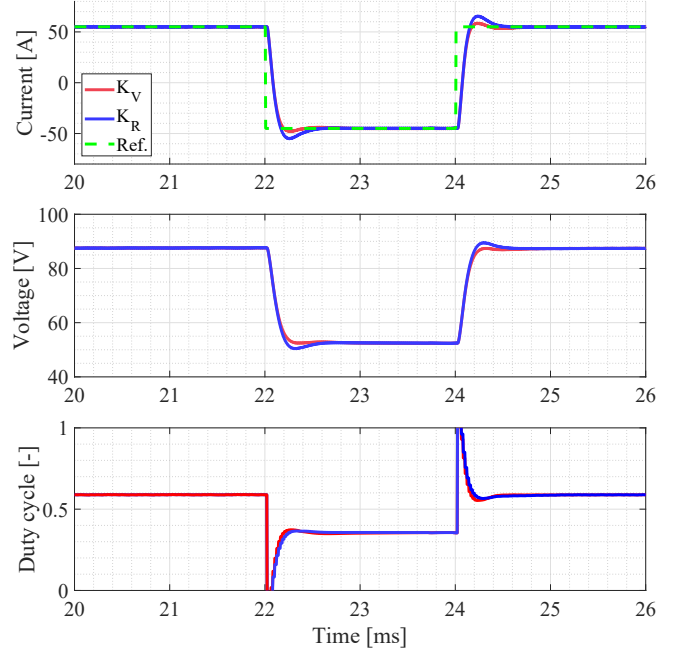


Fig. 5. Output current tracking performance of the two controllers.

TABLE III
COMPARISON OF THE CONTROLLER PERFORMANCE METRICS FOR
THE TWO TUNED CONTROLLERS

	Settling time [ms (%)]	Overshoot [%]
$K_V(z)$	0.35 (17)	5
$K_R(z)$	0.55 (28)	17

The plant used for simulation consists of the bidirectional BBC using IGBT for switches, which is supplying the RSOEC represented by the Voigt ECM. For the two designed controllers the output current tracking performance for the cyclic reference is investigated. The cyclic output current reference amplitude is set to 55A in electrolysis mode and 45A in fuel cell mode and the frequency to a maximum 50 Hz and the percentage of electrolysis to fuel cell operating time is set to a maximum of 90%. In Fig. 5 the tracking performance of the two discrete controllers can be seen at a single cyclic operation jump. By comparing the two controllers response, the controller K_V achieves a less transient oscillation, a much lower overshoot, and a slightly reduced settling time. The performance metrics extracted from the simulation for the two controllers can be numerically compared in Table III. It can be concluded that the initial design requirements for the maximum settling time and overshoot was fulfilled for the controller tuned using the Voigt ECM, whereas the controller tuned using the Resistive ECM do not fulfil these.

VI. CONCLUSION

This paper initially presents a novel investigation of the requirements for a bidirectional DC-DC converter and the associated control system for enabling the cyclic operation of an RSOEC stack. It is determined that for the bidirectional power electronic converter topology and control system, the well-established bidirectional BBC and PIDF control algorithm are suitable. The control design for the PIDF algorithm was carried out in the frequency domain, utilizing Bode plots based on the provided mathematical models of the BBC and RSOEC stack. Two different ECMs were used to represent the electrical behavior of the RSOEC stack in the analysis. The performance of the converter systems was tested through simulations, and it was found that using the Voigt ECM to represent the electrical behavior of the RSOEC in the control design gave a better performance than using the simple Resistive ECM. Furthermore, by using the Voigt ECM for the control design, the converter system was able to fulfill the control design requirements. This paper shows a straightforward method for the design of a baseline bidirectional DC-DC power electronic converter system enabling the cyclic operation of an RSOEC stack using well-established methods. Additionally, it is essential to conduct further research on various bidirectional DC-DC power electronic converters and control methodologies. The objective is to maximize the performance, robustness, efficiency, and applicability for large-scale RSOEC plants by conducting research and implementing improvements.

REFERENCES

- [1] A. Buttler and H. Spliethoff, "Current status of water electrolysis for energy storage, grid balancing and sector coupling via power-to-gas and power-to-liquids: A review," *Renewable and Sustainable Energy Reviews*, vol. 82, no. September 2017, pp. 2440–2454, 2018. [Online]. Available: <https://dx.doi.org/10.1016/j.rser.2017.09.003>
- [2] A. Hauch, R. Küngas, P. Blennow, A. B. Hansen, J. B. Hansen, B. V. Mathiesen, and M. B. Mogensen, "Recent advances in solid oxide cell technology for electrolysis," *Science*, vol. 370, no. 6513, p. eaba6118, oct 2020. [Online]. Available: <https://dx.doi.org/10.1126/science.aba6118>
- [3] C. Graves, S. D. Ebbesen, S. H. Jensen, S. B. Simonsen, and M. B. Mogensen, "Eliminating degradation in solid oxide electrochemical cells by reversible operation," *Nature Materials*, vol. 14, no. 2, pp. 239–244, 2015.
- [4] T. L. Skafte, O. B. Rizvandi, A. L. Smitshuysen, H. L. Frandsen, J. V. Thorvald Høgh, A. Hauch, S. K. Kær, S. S. Araya, C. Graves, M. B. Mogensen, and S. H. Jensen, "Electrothermally balanced operation of solid oxide electrolysis cells," *Journal of Power Sources*, vol. 523, 2022. [Online]. Available: <http://dx.doi.org/10.10810.1016/j.jpowsour.2022.231040>
- [5] S. A. Gorji, H. G. Sahebi, M. Ektesabi, and A. B. Rad, "Topologies and control schemes of bidirectional DC-DC power converters: An overview," *IEEE Access*, vol. 7, pp. 117997–118019, 2019.
- [6] V. Fernão Pires, E. Romero-Cadaval, D. Vinnikov, I. Roasto, and J. F. Martins, "Power converter interfaces for electrochemical energy storage systems - A review," *Energy Conversion and Management*, vol. 86, pp. 453–475, 2014.
- [7] M. Zhang and W. Zheng, "Refined Modeling and Bi-directional Power Flow Control of Reversible Solid Oxide Cell," *2021 IEEE 2nd China International Youth Conference on Electrical Engineering, CIYCEE 2021*, pp. 1–7, 2021.
- [8] R. J. Wai and B. H. Chen, "High-efficiency dual-input interleaved DC-DC converter for reversible power sources," *IEEE Transactions on Power Electronics*, vol. 29, no. 6, pp. 2903–2921, 2014.
- [9] R. Pittini, Z. Zhang, and M. A. Andersen, "Analysis of DC/DC converter efficiency for energy storage system based on bidirectional fuel cells," *2013 4th IEEE/PES Innovative Smart Grid Technologies Europe, ISGT Europe 2013*, pp. 2011–2014, 2013.
- [10] —, "Isolated full bridge boost DC-DC converter designed for bidirectional operation of fuel cells/electrolyzer cells in grid-tie applications," *2013 15th European Conference on Power Electronics and Applications, EPE 2013*, 2013.
- [11] R. Pittini, M. C. Mira, Z. Zhang, A. Knott, and M. A. Andersen, "Analysis and comparison based on component stress factor of dual active bridge and isolated full bridge boost converters for bidirectional fuel cells systems," *Proceedings - 2014 International Power Electronics and Application Conference and Exposition, IEEE PEAC 2014*, pp. 1026–1031, 2014.
- [12] Y. Xiao, Z. Zhang, M. A. Andersen, and B. Engelbrecht Thomsen, "Partial parallel dual active bridge converter with variable voltage gain for SOEC/SOFC system," *Conference Proceedings - IEEE Applied Power Electronics Conference and Exposition - APEC*, vol. 2019-March, pp. 1641–1646, 2019.
- [13] W. Kong, K. Qu, X. Lin, K. Sun, S. Mu, and Y. Zhou, "Loss Comparison of Two Bidirectional Isolated DC/DC Converters for Reversible Solid Oxide Fuel Cell Systems," *Proceedings - 2018 IEEE International Power Electronics and Application Conference and Exposition, PEAC 2018*, 2018.
- [14] X. Lin, K. Sun, J. Lin, Z. Zhang, and W. Kong, "A Multi-Port Bidirectional Power Conversion System for Reversible Solid Oxide Fuel Cell Applications," *2018 International Power Electronics Conference, IPEC-Niigata - ECCE Asia 2018*, pp. 3460–3465, 2018.
- [15] H. Chong, K. Sun, and H. Chen, "A Power Conversion System for Large-Scale Reversible SOFC Energy Storage System," *2021 6th IEEE Workshop on the Electronic Grid, eGRID 2021*, 2021.
- [16] J. Hong, H.-j. Kim, S.-y. Park, J.-h. Lee, S.-b. Park, J.-h. Lee, B.-k. Kim, H.-j. Je, J. Yuk, and K. Joong, "Electrochemical performance and long-term durability of a 200 W-class solid oxide regenerative fuel cell stack," *International Journal of Hydrogen Energy*, vol. 39, no. 35, pp. 20819–20828, 2014. [Online]. Available: <http://dx.doi.org/10.1016/j.ijhydene.2014.06.114>
- [17] M. Meiler, O. Schmid, M. Schudy, and E. P. Hofer, "Dynamic fuel cell stack model for real-time simulation based on system identification," *Journal of Power Sources*, vol. 176, no. 2, pp. 523–528, 2008.
- [18] K. Tomas-Manez, A. Anthon, and Z. Zhang, "High efficiency power converter for a doubly-fed SOEC/SOFC system," *Conference Proceedings - IEEE Applied Power Electronics Conference and Exposition - APEC*, vol. 2016-May, pp. 1235–1242, 2016.
- [19] K. Jessen, M. Soltani, A. Hajizadeh, S. H. Jensen, E. Schaltz, M. N. Nielsen, and T. E. L. Smitshuysen, "Grey-box modeling of reversible solid oxide cell stack's electrical dynamics based on electrochemical impedance spectroscopy [unpublished, accepted]," *Proc. IEEE Conf. Control Technol. Appl. (CCTA)*, 2023.
- [20] V. Grigore, J. Hatonen, J. Kyyra, and T. Suntio, "Dynamics of a buck converter with a constant power load," in *PESC Record - IEEE Annual Power Electronics Specialists Conference*, vol. 1, 1998, pp. 72–78.
- [21] R. D. Middlebrook and S. Cuk, "A general unified approach to modelling switching-converter power stages," in *1976 IEEE Power Electronics Specialists Conference*, vol. 21, no. 1. IEEE, jun 1976, pp. 18–34. [Online]. Available: <https://ieeexplore.ieee.org/document/7072895/>
- [22] X. Yue, X. Wang, and F. Blaabjerg, "Review of Small-Signal Modeling Methods Including Frequency-Coupling Dynamics of Power Converters," *IEEE Transactions on Power Electronics*, vol. 34, no. 4, pp. 3313–3328, 2019.